Merger rate of supermassive primordial black hole binaries

Hai-Long Huang [1,*] Jun-Qian Jiang [1,†] and Yun-Song Piao [1,2,3,4,‡]

[1] *School of Physical Sciences, University of Chinese Academy of Sciences, Beijing 100049, China*
[2] *International Center for Theoretical Physics Asia-Pacific, Beijing/Hangzhou 100190, China*
[3] *School of Fundamental Physics and Mathematical Sciences, Hangzhou Institute for Advanced Study, UCAS, Hangzhou 310024, China*
[4] *Institute of Theoretical Physics, Chinese Academy of Sciences, P.O. Box 2735, Beijing 100190, China*

(Received 10 December 2023; accepted 20 February 2024; published 11 March 2024)

The probability that the primordial black hole (PBH) binaries formed in the early Universe can be affected by the Hubble expansion of background, which is non-negligible when the number density of PBHs is very low (it is actually this case for supermassive PBHs). In this paper, taking into account the effect of cosmic expansion on the comoving distance of PBH pairs, we worked out the merger rate of PBHs with any extended mass function. The torques by all PBHs and linear density perturbations are also considered. It is found that the merger rate of PBH, $M \gtrsim 10^6 M_\odot$, binaries is significantly lower for $f_{\rm pbh} \lesssim 0.01$ than expected.

DOI: 10.1103/PhysRevD.109.063515

I. INTRODUCTION

Recently, the detection by LIGO/Virgo of the gravitational waves (GWs) emitted by the merging of black hole (BH) binaries, $M \sim 10 M_\odot$ (e.g., [1,2]) has revived the interest in the models of PBHs [3–5], although other explanations for the origins of such BHs as well as the LIGO/Virgo binaries are also possible (see e.g., Ref. [6]). It has been widely thought that PBHs can constitute a fraction of or all dark matter [7–9].

The nanohertz stochastic GW background (SGWB) detected recently by pulsar timer array experiments [10–13] might be interpreted with a population of supermassive BH binaries with $M \gtrsim 10^9 M_\odot$ [14–16]. The developing space-based detectors, e.g., LISA [17] and Taiji [18], which aim for mHz GWs, are ideal for detecting the mergers of massive and supermassive BHs with masses above $10^3 M_\odot$, e.g., [19]. Supermassive BHs also may have primordial inflationary origin (e.g., [20], see also [21,22]), i.e., supermassive PBHs (SMPBHs). It is well-known that the result of the merger rate of PBHs is necessary for assessing the event rate of PBH mergers at different redshift, which might be significant for distinguishing PBHs from astrophysical BHs, and SGWB.

There are some earlier works on the merger rate of PBHs, which were effectively randomly distributed in space and formed in the early Universe.[1] The merger rate of PBHs in Refs. [9,29] is applicable to the case that all PBHs have the same (monochromatic) mass and the torque is exerted only by the nearest PBH. In Ref. [28], the tidal torquing by all other PBHs, as well as standard large-scale adiabatic perturbations, has also been taken into account (see also [30,31] for the extended mass function). References [32,33] also presented the merger rate of PBHs with nonmonochromatic mass. Though N-body simulations have been performed in Ref. [33], the mass range of PBHs simulated is $\sim \mathcal{O}(10) M_\odot$.

However, when the number density of PBHs is very low (it is actually this case for SMPBHs), the effect of cosmic Hubble expansion on binding PBH binaries (specifically, on the comoving separation of PBH pair)[2] so the merger rate might be not negligible. Relevant studies, e.g., Refs. [28,30,31], did not take this effect into account. The current observations require the fraction of PBHs $f_{\rm pbh} \lesssim 10^{-3}$ for $10^6 M_\odot \lesssim M \lesssim 10^{12} M_\odot$, thus the number density $\sim \rho_{\rm pbh} M^{-1}$ is actually considerably low for SMPBHs.

In this paper, taking into account the effect of cosmic expansion on comoving separation of PBH pairs, we show our merger rate in Sec. II and discuss its implications in Sec. III. Throughout this paper we use units $c = G = 1$ and the values of cosmological parameters are set in light of the Planck results [34]. We denote by t_0 the present time. The scale factor is normalized to unity at the matter radiation equality $z = z_{\rm eq} \approx 3400$.

[*] huanghailong18@mails.ucas.ac.cn
[†] jiangjq2000@gmail.com
[‡] yspiao@ucas.ac.cn

[1] Conversely, see e.g., [23–26] for an initially clustered spatial distribution and [7,27,28] for the merger rate in the late Universe.

[2] The physical distance of PBH pair at the decoupling time is equal to the semimajor axis of the resultant binary [32]; this can be converted to the maximum for the semimajor axis as in Ref. [29].

II. MERGER RATE

The probability distribution function of PBHs, as described in Refs. [33,35,36], is defined as

$$\psi(m) \equiv \frac{m}{\rho_{\rm pbh}} \frac{\mathrm{d}n}{\mathrm{d}m}, \tag{1}$$

with $\psi(m)$ normalized as $\int \psi(m)\mathrm{d}m = 1$, where $\rho_{\rm pbh}$ is the energy density of PBHs and $n(m)$ is the average number density of PBHs in the mass interval $(m, m + \mathrm{d}m)$.

The comoving total average number density of PBHs is

$$n_T = \frac{\rho_{\rm pbh}}{\langle m \rangle}, \tag{2}$$

where $\langle m \rangle \equiv \frac{1}{n} \int m \mathrm{d}n = (\int \mathrm{d}m \frac{\psi(m)}{m})^{-1}$ is the mean mass of PBHs with $n = \int \mathrm{d}n(m)$. The fraction of the average number density of PBHs in the total average number density of PBHs is [31,37]

$$F(m) \equiv \frac{n(m)}{n_T} = \psi(m) \frac{\langle m \rangle}{m}. \tag{3}$$

Additionally, the characteristic comoving separation between the nearest PBH pairs, labeled as m_i and m_j, is determined by [28] as follows:

$$\bar{x} = \left(\frac{3}{4\pi n_T}\right)^{1/3}. \tag{4}$$

We denote by $\rho_{\rm eq}$ the matter density at matter-radiation equality,

$$\rho_{\rm eq} = \rho_{m,0}(1 + z_{\rm eq})^3, \tag{5}$$

where $\rho_{m,0}$ is the matter density at present. Then the comoving energy density of PBH is $\rho_{\rm pbh} = f\rho_{\rm eq}$, with $f \equiv \rho_{\rm pbh}/\rho_m \approx 0.85 f_{\rm pbh}$ is the total abundance of PBHs in nonrelativistic matter, while $f_{\rm pbh} \equiv \rho_{\rm pbh}/\rho_{\rm dm}$ is the fraction of PBHs in dark matter. The energy density of radiation in the radiation era is

$$\rho_r(z) = \rho_{\rm eq}\left(\frac{1+z}{1+z_{\rm eq}}\right)^4. \tag{6}$$

The condition for two PBHs to become gravitationally bound is that the total energy $m_i + m_j$ of PBHs must exceed the background energy contained in the comoving bulk to the nearest PBH [32], i.e.,

$$m_i + m_j > \frac{8\pi}{3}\left(x \cdot \frac{1+z_{\rm eq}}{1+z}\right)^3 \rho(z), \tag{7}$$

where x is the comoving separation (i.e., the proper separation at $z_{\rm eq}$) of the PBH pair. It is expected that only when

$$x < x_{\rm max} = \left(\frac{3}{8\pi} \cdot \frac{m_i + m_j}{\rho_{\rm eq}}\right)^{1/3}, \tag{8}$$

can the PBH pair come into being at redshift $z = z_{\rm dec} > z_{\rm eq}$ with

$$1 + z_{\rm dec} = (1 + z_{\rm eq})\left(\frac{x_{\rm max}}{x}\right)^3. \tag{9}$$

By solving the equation of motion for the proper separation projected along the axis of motion of PBH pair numerically, one can get the semimajor axis a of the binary [28],

$$a \approx 0.1\lambda x, \tag{10}$$

with

$$\lambda = \frac{8\pi\rho_{\rm eq}x^3}{3(m_i + m_j)} = \left(\frac{x}{x_{\rm max}}\right)^3 < 1. \tag{11}$$

Equation (10) also shows that the semimajor axis is equivalent to the physical distance of the PBH pair at the decoupling time numerically, i.e., $a \sim x(1 + z_{\rm eq})/(1 + z_{\rm dec})$ [32].

In the case of sparse PBH distribution, the condition $x < x_{\rm max}$ (or equivalently, $\lambda < 1$) must be taken into account in the probability distribution $P(m_i, m_j, x)$ of x between two nearest PBHs with masses m_i and m_j (but without other PBHs in the bulk of $4\pi x^3/3$). Assuming a random distribution for PBHs, we derive the following expression:

$$\begin{aligned} \mathrm{d}P(m_i, m_j, X) &= 4\pi x^2 \Theta(x_{\rm max} - x)\mathrm{d}x \left[F(m_i)\mathrm{d}m_i n(m_j)\mathrm{d}m_j e^{\frac{-4\pi x^3 n(m_j)\mathrm{d}m}{3}} \prod_{m \neq m_j} e^{\frac{-4\pi x^3 n(m)\mathrm{d}m}{3}}\right] \\ &= \Theta(X_{\rm max} - X)\mathrm{d}X F(m_i)\mathrm{d}m_i F(m_j)\mathrm{d}m_j e^{-X}, \end{aligned} \tag{12}$$

where $X \equiv (x/\bar{x})^3 = 4\pi n_T x^3/3$, with

$$X_{\max} \equiv \left(\frac{x_{\max}}{\bar{x}}\right)^3 = \frac{(m_i + m_j)n_T}{2\rho_{\rm eq}}. \tag{13}$$

Then we need to calculate the dimensionless angular momentum j of the PBH pair with the torque by all surrounding PBHs and density perturbations of the rest dark matter. The probability distribution of j for a given X is

$$j\frac{\mathrm{d}P}{\mathrm{d}j}\bigg|_X = \mathcal{P}(j/j_X), \qquad \mathcal{P}(\gamma) \equiv \frac{\gamma^2}{(1+\gamma^2)^{3/2}}, \tag{14}$$

see e.g., Refs. [28,30,31] for detailed derivation, where the characteristic value of j_X is estimated as [31]

$$j_X \approx \frac{\langle m\rangle}{m_i + m_j}(1 + \sigma_{\rm eq}^2/f^2)^{1/2} X. \tag{15}$$

Here $\sigma_{\rm eq}^2$ is the variance of density perturbations of the rest of dark matter at $z_{\rm eq}$ [28]. As a comparison, the angular momentum only accounting for tidal torquing by the nearest PBH with mass of m_l (the comoving distance is x') is estimated as [38,39]

$$j \sim \frac{2m_l}{m_i + m_j}\left(\frac{x}{x'}\right)^3, \tag{16}$$

which is physically natural only for a (or nearly) monochromatic mass function. However, since the torque is also proportional to the mass of the outer PBH, Eq. (16) is not valid if the mass of PBHs extends over many orders of magnitude. Thus, we adopt Eq. (14).

The angular momentum j can be expressed by the semimajor axis a and the coalescence time t as [40]

$$j = \left[\frac{85}{3}\cdot\frac{m_i m_j (m_i + m_j)}{a^4}\right]^{1/7} t^{1/7}. \tag{17}$$

Then we have

$$\gamma_X = \frac{j(t;X)}{j_X} = C t^{1/7} X^{-37/21}. \tag{18}$$

The factor C only depends on m_i and m_j. Combining Eqs. (12), (14), (15), and (17), we can get the probability distribution of the merger time

$$\begin{aligned}\frac{\mathrm{d}P(m_i, m_j, X)}{\mathrm{d}t} &= \int \mathrm{d}X \frac{\mathrm{d}^2 P(m_i, m_j, X)}{\mathrm{d}X\mathrm{d}t} \\ &= \frac{1}{7t} F(m_i)\mathrm{d}m_i F(m_j)\mathrm{d}m_j \\ &\quad \times \int \mathrm{d}X e^{-X}\Theta(X_{\max} - X)\mathcal{P}(\gamma_X).\end{aligned} \tag{19}$$

The peak of $\mathcal{P}(\gamma_X)$ is at $X_* \ll 1$, see Appendix A, which suggests that $e^{-X} \approx 1$ in Eq. (19) [28,30,31]. Thus, with the generalized hypergeometric function ${}_2F_1$, the integral in Eq. (19) can be integrated out as

$$\begin{aligned}\int \mathrm{d}X\Theta(X_{\max} - X)\mathcal{P}(\gamma_X) = \frac{21 X_{\max}^{58/21}}{2146(C^2 t^{2/7} + X_{\max}^{74/21}) C t^{1/7}} \Bigg[& 95 C^2 t^{2/7} {}_2F_1\left(-\frac{1}{2}, \frac{29}{37}, \frac{66}{37}, -\frac{X_{\max}^{74/21}}{C^2 t^{2/7}}\right) \\ & - (58 C^2 t^{2/7} + 21 X_{\max}^{74/21}) {}_2F_1\left(\frac{1}{2}, \frac{29}{37}, \frac{66}{37}, -\frac{X_{\max}^{74/21}}{C^2 t^{2/7}}\right)\Bigg].\end{aligned} \tag{20}$$

It is convenient to rewrite Eq. (20) as $\int \mathrm{d}X\Theta(X_{\max} - X)\mathcal{P}(\gamma_X) = X_{\max} Y(y)$ with

$$Y(y) = \frac{21y}{2146(1+y^2)}\left[95\,{}_2F_1\left(-\frac{1}{2}, \frac{29}{37}, \frac{66}{37}, -y^2\right) - (58 + 21y^2)\,{}_2F_1\left(\frac{1}{2}, \frac{29}{37}, \frac{66}{37}, -y^2\right)\right], \tag{21}$$

where

$$\begin{aligned}y(m_i, m_j, t) &\equiv \frac{1}{\gamma_X(t; X_{\max})} = \frac{X_{\max}^{37/21}}{C t^{1/7}} \\ &\approx 2.95 \times 10^2 f \left(1 + \frac{\sigma_{\rm eq}^2}{f^2}\right)^{\frac{1}{2}} \left(\frac{m_i}{M_\odot}\right)^{-\frac{1}{7}} \left(\frac{m_j}{M_\odot}\right)^{-\frac{1}{7}} \left(\frac{m_i + m_j}{M_\odot}\right)^{\frac{1}{21}} \left(\frac{t}{t_0}\right)^{-\frac{1}{7}}.\end{aligned} \tag{22}$$

Thus, our resulting merger rate is

$$R(t) = \frac{\mathrm{d}N_{\rm merge}}{\mathrm{d}t\mathrm{d}V} = \frac{1}{2}\frac{n_T}{(1+z_{\rm eq})^3}\frac{\mathrm{d}P}{\mathrm{d}t} \equiv \iint \mathcal{R}(m_i, m_j, t)\mathrm{d}m_i\mathrm{d}m_j, \tag{23}$$

where $\mathcal{R}(m_i, m_j, t)$ is the differential merger rate,

$$\mathcal{R}(m_i, m_j, t) \approx \frac{1.02 \times 10^8}{\mathrm{Gpc}^3\ \mathrm{yr}} f^2 \left(\frac{m_i}{M_\odot}\right)^{-1} \left(\frac{m_j}{M_\odot}\right)^{-1} \left(\frac{m_i + m_j}{M_\odot}\right) \left(\frac{t}{t_0}\right)^{-1} Y(y(m_i, m_j, t)) \psi(m_i) \psi(m_j). \tag{24}$$

III. IMPLICATION OF OUR MERGER RATE

In the condition that the number density of PBHs is large, resulting in $y \geq 1$ according to Eq. (22) and $Y(y) \approx 0.42 y^{-0.54}$, see Fig. 1. After substituting $Y(y)$ into Eq. (24) combined with Eq. (22), we arrive that

$$\mathcal{R}(m_i, m_j, t) \approx \frac{1.99 \times 10^6}{\mathrm{Gpc}^3\ \mathrm{yr}} f^{1.46} \left(1 + \frac{\sigma_{\mathrm{eq}}^2}{f^2}\right)^{-0.27} \left(\frac{m_i}{M_\odot}\right)^{-0.92} \left(\frac{m_j}{M_\odot}\right)^{-0.92} \left(\frac{m_i + m_j}{M_\odot}\right)^{0.97} \left(\frac{t}{t_0}\right)^{-0.92} \psi(m_i) \psi(m_j). \tag{25}$$

Equation (25) corresponds to the merger rate without the limitation $X < X_{\max}$, i.e., the effect of cosmic expansion on the comoving distance of PBH pairs is negligible. In, e.g., Ref. [31], such a merger rate density has been calculated as follows:

$$\mathcal{R}_{\mathrm{no-expan}}(m_i, m_j, t) = \frac{1.94 \times 10^6}{\mathrm{Gpc}^3 \mathrm{yr}} f^{\frac{53}{37}} \left(1 + \frac{\sigma_{\mathrm{eq}}^2}{f^2}\right)^{-\frac{21}{74}} \left(\frac{m_i}{M_\odot}\right)^{-\frac{34}{37}} \left(\frac{m_j}{M_\odot}\right)^{-\frac{34}{37}} \left(\frac{m_i + m_j}{M_\odot}\right)^{\frac{36}{37}} \left(\frac{t}{t_0}\right)^{-\frac{34}{37}} \psi(m_i) \psi(m_j), \tag{26}$$

which is essentially consistent with our Eq. (25).

Now let us consider the typical PBH mass functions specifically. Taking the monochromatic PBHs,

$$\psi(m) = \delta(m - M), \tag{27}$$

we plot $R(t_0)$ and $R_{\mathrm{no-expan}}(t_0)$ for different $M = 10 M_\odot, 10^3 M_\odot, 10^6 M_\odot$ in Fig. 2, respectively. As expected, we always observe $R(t) \lesssim R_{\mathrm{no-expan}}(t)$. Furthermore, the smaller the value of M or the larger the value of f_{pbh}, the closer these two merger rates become. This implies that neglecting the effect of cosmic expansion on the separation can only be considered safe when the number density of PBHs, $\sim \rho_{\mathrm{pbh}} M^{-1}$, is very high.

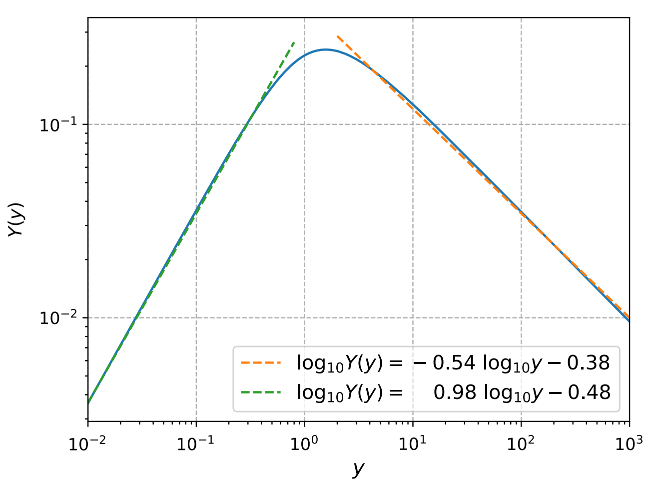

FIG. 1. $Y(y)$ with respect to y according to Eq. (21).

It is also interesting to consider that of PBHs sourced by supercritical bubbles that nucleated during slow-roll inflation, see Appendix B,

$$\psi(m) = e^{-\sigma^2/8} \sqrt{\frac{M_c}{2\pi\sigma^2 m^3}} \exp\left(-\frac{\ln^2(m/M_c)}{2\sigma^2}\right). \tag{28}$$

In Fig. 3, we plot $R(t)$ and $R_{\mathrm{no-expan}}(t)$ at different redshifts, respectively. It is clearly seen that when

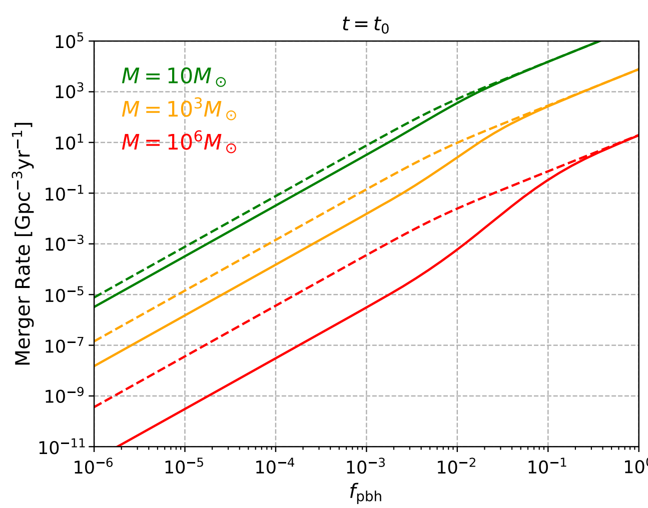

FIG. 2. Merger rate $R(t_0)$ at present of monochromatic PBH binaries with masses $10 M_\odot$ (green), $10^3 M_\odot$ (orange) and $10^6 M_\odot$ (red), respectively. As a comparison, we use different merger rate formulas, i.e., Eqs. (24) (our work, solid lines) and (26) (dashed lines).

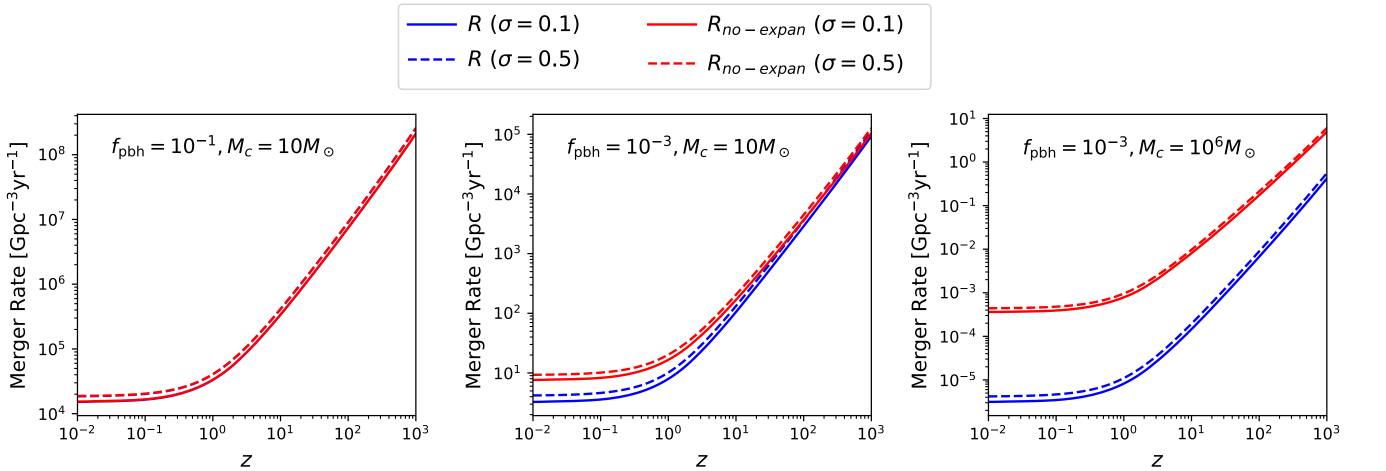

FIG. 3. Merger rate of PBHs (sourced by supercritical bubbles) with an extended mass function Eq. (28) with respect to the redshift according to Eqs. (24) (blue, our work) and (26) (red, Ref. [31]).

$f_{\rm pbh} = 10^{-1}$ and the characteristic mass $M_c = 10 M_\odot$, the difference between $R(t)$ and $R_{\rm no-expan}(t)$ is indistinguishable. However, when $f_{\rm pbh} \sim 10^{-3}$, especially at low redshifts, the difference becomes more pronounced. This is attributed to later binary mergers corresponding to larger separations x, where the effect of cosmic expansion becomes more significant. As a result, the effect of cosmic expansion significantly suppresses the merger rate for SMPBHs.

IV. CONCLUSION

In the early Universe the probability that the PBHs formed might be affected by the Hubble expansion of background, which is non-negligible when the spatial distribution of PBHs is sparse, specially for SMPBHs. In this paper, taking the effect of cosmic expansion on the comoving separation of PBH pair into account, we worked out the merger rate of PBHs with the extended mass function, see Eq. (24). It is found that the merger rate of SMPBHs, $M \gtrsim 10^6 M_\odot$, can be significantly suppressed for $f_{\rm pbh} \lesssim 0.01$.[3]

Throughout our estimation, the subdominant effects, such as the effects of the tidal field from the smooth halo, the encountering with other PBHs, the baryon accretion, present-day halos and the spin of PBHs, are neglected. In order to study the corresponding effects thoroughly, it might be better to perform the N-body simulation in an expanding background. Nonetheless, for the merger of PBHs with any extended mass function, our Eq. (24) might suffice to capture the essential impact of cosmic expansion on the merger rate, which thus can have interesting applications, specially for SMPBHs and low-frequency GWs.

[3]Current cosmological and astrophysical constraints for the abundance of SMPBHs are $f_{\rm pbh} \lesssim 10^{-3}$ [41].

ACKNOWLEDGMENTS

We thanks Yong Cai, Lang Liu and Jun Zhang for helpful discussion. Y. S. P. is supported by NSFC, No. 12075246, National Key Research and Development Program of China, No. 2021YFC2203004, and the Fundamental Research Funds for the Central Universities.

APPENDIX A: ON X_* AND $X_{\rm max}$

The value of X_* maximizes $\mathcal{P}(\gamma_X)$, i.e.,

$$\mathcal{P}'(\gamma_{X_*}) \frac{\partial \gamma_X}{\partial X}\bigg|_{X=X_*} = 0. \quad \text{(A1)}$$

Since γ_X is monotonic, which implies $\mathcal{P}'(\gamma_{X_*}) = 0$, we get

$$j(t; X_*) = \sqrt{2} j_{X_*}, \quad \text{(A2)}$$

According to Eq. (A2) we have

$$X_* \approx 1.63 \times 10^{-2} f^{\frac{16}{37}} \left(1 + \frac{\sigma_{\rm eq}^2}{f^2}\right)^{-\frac{21}{74}} \left(\frac{m_i}{M_\odot}\right)^{\frac{3}{37}} \left(\frac{m_j}{M_\odot}\right)^{\frac{3}{37}} \times \left(\frac{m_i + m_j}{M_\odot}\right)^{\frac{36}{37}} \left(\frac{\langle m \rangle}{M_\odot}\right)^{-1} \left(\frac{t}{t_0}\right)^{\frac{3}{37}}. \quad \text{(A3)}$$

In the monochromatic mass approximation, Eq. (27), we have $X_{\rm max} = f$. Thus,

$$X_* \approx 3.20 \times 10^{-2} f^{\frac{16}{37}} \left(1 + \frac{\sigma_{\rm eq}^2}{f^2}\right)^{-\frac{21}{74}} \left(\frac{M}{M_\odot}\right)^{\frac{5}{37}} \left(\frac{t}{t_0}\right)^{\frac{3}{37}}. \quad \text{(A4)}$$

We plot X_* compared with 1 and $X_{\rm max} = f$ in Fig. 4, which shows that $X_* \ll 1$ in all cases while $X_* > X_{\rm max}$ for SMPBHs.

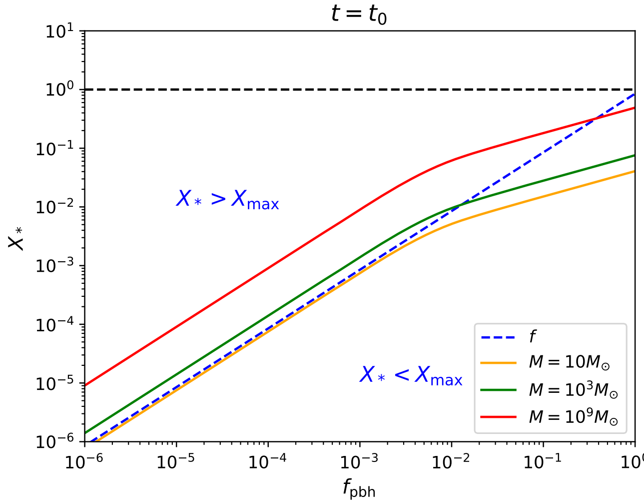

FIG. 4. The most probable value of X for binaries merging today for the PBH population with monochromatic mass function. One can compare it with Fig. 2 in [28]. The blue dotted line represents $X_{\rm max} = f$, above which is the parameter space satisfying $X_* > X_{\rm max}$. We can see that $X_* \ll 1$ still holds in the case of SMPBHs, considering the cosmological and astrophysical constraints on the abundance for SMPBHs [42,43] (e.g., we have $f_{\rm pbh} < 10^{-3}$ for $M = 10^9 M_\odot$). Thus, it is safe to neglect the factor e^{-X} in Eq. (19). However, we do not have $X_* \ll X_{\rm max}$ similarly, especially for SMPBHs. Here, $\sigma_{\rm eq} = 0.005$.

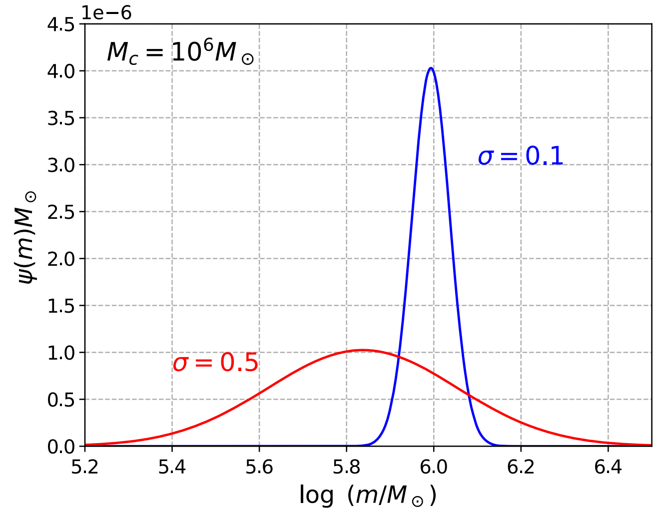

FIG. 5. The normalized mass function of PBHs sourced by supercritical bubbles.

APPENDIX B: MASS DISTRIBUTION OF PBHs SOURCED BY SUPERCRITICAL BUBBLES

The bubbles that nucleated during slow-roll inflation can naturally develop to the PBHs [44,45]. It is found in Ref. [20][4] that the PBHs sourced by supercritical bubbles not only can be supermassive, $M \gtrsim 10^9 M_\odot$, but also have a peaklike mass function[5]

$$\psi(m) \sim \frac{(c_1 c_2^3)^{\frac{1}{2}}}{f_{\rm pbh} M_\odot} \exp\{-B_*[1 + c_3(\mathcal{N}^{1/2} - \mathcal{N}_*^{1/2})^2]^{n/2} - 3\mathcal{N}\}, \tag{B1}$$

with $c_1 = \mathcal{M}_{\rm eq}/M_\odot \approx 10^{17}$, $c_2 = H_i M_\odot / M_p^2 \approx 10^{32}$, and $\mathcal{N} = \ln \sqrt{c_2(m/M_\odot)}$, where $n = 1$ for the nucleation of the domain wall [44,49] and $n = 4$ for the vacuum bubble [50], H_i is the inflationary Hubble parameter, $\mathcal{N}$ is the e-folds number before inflation ended. In corresponding model, we naturally have the parameters $c_3 \gg 1$, $B_* \sim \mathcal{O}(10)$, and $\mathcal{N}_* \sim \mathcal{O}(10)$.

It is convenient to convert $\mathcal{N}_*$ to the characteristic mass M_c by

$$\mathcal{N}_* \equiv \ln \sqrt{c_2(M_c/M_\odot)}. \tag{B2}$$

In the approximation of $\mathcal{N} \to \mathcal{N}_*$ (or equivalently, $m \to M_c$), we have

$$\psi(m) \propto \frac{1}{m^{3/2}} \exp\left\{-B_*\left[1 + c_3 \frac{\ln^2(m/M_c)}{16\mathcal{N}_*}\right]^{n/2}\right\} \sim \frac{1}{m^{3/2}} \exp\left[-B_*\left(1 + \frac{\ln^2(m/M_c)}{2\sigma^2}\right)\right], \tag{B3}$$

where $\sigma \equiv 4\sqrt{\mathcal{N}_*/(nc_3)}$ corresponds to the width of mass peak. Thus, the normalized mass function is

$$\psi(m) = e^{-\sigma^2/8} \sqrt{\frac{M_c}{2\pi\sigma^2 m^3}} \exp\left(-\frac{\ln^2(m/M_c)}{2\sigma^2}\right). \tag{B4}$$

It is obvious that $\psi(m)$ approaches the monochromatic spectrum centered on M_c as $\sigma \to 0$, see Fig. 5. According to Eq. (B4), we have

$$\langle m \rangle = M_c e^{-\sigma^2} \quad \text{and} \quad \langle m^2 \rangle = M_c^2 e^{-\sigma^2}. \tag{B5}$$

[4]Here, the nucleating rate of bubbles must satisfy $\lambda \ll 1$. In the case of $\lambda \gtrsim 1$, the resulting scenario corresponds to a two-stage inflation model with an intermediate first-order phase transition, during which the collisions between bubbles that nucleated will contribute inflationary GWB, e.g., [46,47].

[5]See also Ref. [48] for a different perspective.

[1] B. P. Abbott *et al.* (LIGO Scientific and Virgo Collaborations), Observation of gravitational waves from a binary black hole merger, Phys. Rev. Lett. **116**, 061102 (2016).

[2] B. P. Abbott *et al.* (LIGO Scientific and Virgo Collaborations), GW151226: Observation of gravitational waves from a 22-solar-mass binary black hole coalescence, Phys. Rev. Lett. **116**, 241103 (2016).

[3] Y. B. Zel'dovich and I. D. Novikov, The hypothesis of cores retarded during expansion and the hot cosmological model, Sov. Astron. AJ (Engl. Transl.), **10**, 602 (1967).

[4] S. Hawking, Gravitationally collapsed objects of very low mass, Mon. Not. R. Astron. Soc. **152**, 75 (1971).

[5] B. J. Carr and S. W. Hawking, Black holes in the early Universe, Mon. Not. R. Astron. Soc. **168**, 399 (1974).

[6] B. P. Abbott *et al.* (LIGO Scientific and Virgo Collaborations), Astrophysical implications of the binary black-hole merger GW150914, Astrophys. J. Lett. **818**, L22 (2016).

[7] S. Bird, I. Cholis, J. B. Muñoz, Y. Ali-Haïmoud, M. Kamionkowski, E. D. Kovetz, A. Raccanelli, and A. G. Riess, Did LIGO detect dark matter?, Phys. Rev. Lett. **116**, 201301 (2016).

[8] S. Clesse and J. García-Bellido, The clustering of massive primordial black holes as dark matter: Measuring their mass distribution with Advanced LIGO, Phys. Dark Universe **15**, 142 (2017).

[9] M. Sasaki, T. Suyama, T. Tanaka, and S. Yokoyama, Primordial black hole scenario for the gravitational-wave event GW150914, Phys. Rev. Lett. **117**, 061101 (2016); **121**, 059901(E) (2018).

[10] G. Agazie *et al.* (NANOGrav Collaboration), The NANOGrav 15 yr data set: Evidence for a gravitational-wave background, Astrophys. J. Lett. **951**, L8 (2023).

[11] H. Xu *et al.*, Searching for the nano-hertz stochastic gravitational wave background with the Chinese Pulsar Timing Array Data Release I, Res. Astron. Astrophys. **23**, 075024 (2023).

[12] D. J. Reardon *et al.*, Search for an isotropic gravitational-wave background with the Parkes Pulsar Timing Array, Astrophys. J. Lett. **951**, L6 (2023).

[13] J. Antoniadis *et al.* (EPTA and InPTA Collaborations), The second data release from the European Pulsar Timing Array—III. Search for gravitational wave signals, Astron. Astrophys. **678**, A50 (2023).

[14] G. Agazie *et al.* (NANOGrav Collaboration), The NANOGrav 15 yr data set: Constraints on supermassive black hole binaries from the gravitational-wave background, Astrophys. J. Lett. **952**, L37 (2023).

[15] J. Ellis, M. Fairbairn, G. Hütsi, J. Raidal, J. Urrutia, V. Vaskonen, and H. Veermäe, Gravitational waves from SMBH binaries in light of the NANOGrav 15-year data, Phys. Rev. D **109**, L021302 (2024).

[16] P. F. Depta, K. Schmidt-Hoberg, P. Schwaller, and C. Tasillo, Do Pulsar Timing Arrays observe merging primordial black holes?, arXiv:2306.17836.

[17] P. Amaro-Seoane *et al.* (LISA Collaboration), Laser Interferometer Space Antenna, arXiv:1702.00786.

[18] W.-R. Hu and Y.-L. Wu, The Taiji program in space for gravitational wave physics and the nature of gravity, Natl. Sci. Rev. **4**, 685 (2017).

[19] E. Bagui *et al.* (LISA Cosmology Working Group), Primordial black holes and their gravitational-wave signatures, arXiv:2310.19857.

[20] H.-L. Huang, Y. Cai, J.-Q. Jiang, J. Zhang, and Y.-S. Piao, Supermassive primordial black holes in multiverse: For nano-Hertz gravitational wave and high-redshift JWST galaxies, arXiv:2306.17577.

[21] D. Hooper, A. Ireland, G. Krnjaic, and A. Stebbins, Supermassive primordial black holes from inflation, arXiv:2308.00756.

[22] T. Nakama, T. Suyama, and J. Yokoyama, Supermassive black holes formed by direct collapse of inflationary perturbations, Phys. Rev. D **94**, 103522 (2016).

[23] M. Raidal, V. Vaskonen, and H. Veermäe, Gravitational waves from primordial black hole mergers, J. Cosmol. Astropart. Phys. 09 (2017) 037.

[24] V. Desjacques and A. Riotto, Spatial clustering of primordial black holes, Phys. Rev. D **98**, 123533 (2018).

[25] D. Inman and Y. Ali-Haïmoud, Early structure formation in primordial black hole cosmologies, Phys. Rev. D **100**, 083528 (2019).

[26] V. De Luca, V. Desjacques, G. Franciolini, and A. Riotto, The clustering evolution of primordial black holes, J. Cosmol. Astropart. Phys. 11 (2020) 028.

[27] H. Nishikawa, E. D. Kovetz, M. Kamionkowski, and J. Silk, Primordial-black-hole mergers in dark-matter spikes, Phys. Rev. D **99**, 043533 (2019).

[28] Y. Ali-Haïmoud, E. D. Kovetz, and M. Kamionkowski, Merger rate of primordial black-hole binaries, Phys. Rev. D **96**, 123523 (2017).

[29] M. Sasaki, T. Suyama, T. Tanaka, and S. Yokoyama, Primordial black holes—perspectives in gravitational wave astronomy, Classical Quantum Gravity **35**, 063001 (2018).

[30] Z.-C. Chen and Q.-G. Huang, Merger rate distribution of primordial-black-hole binaries, Astrophys. J. **864**, 61 (2018).

[31] L. Liu, Z.-K. Guo, and R.-G. Cai, Effects of the surrounding primordial black holes on the merger rate of primordial black hole binaries, Phys. Rev. D **99**, 063523 (2019).

[32] B. Kocsis, T. Suyama, T. Tanaka, and S. Yokoyama, Hidden universality in the merger rate distribution in the primordial black hole scenario, Astrophys. J. **854**, 41 (2018).

[33] M. Raidal, C. Spethmann, V. Vaskonen, and H. Veermäe, Formation and evolution of primordial black hole binaries in the early universe, J. Cosmol. Astropart. Phys. 02 (2019) 018.

[34] N. Aghanim *et al.* (Planck Collaboration), Planck 2018 results. VI. Cosmological parameters, Astron. Astrophys. **641**, A6 (2020); **652**, C4(E) (2021).

[35] A. Hall, A. D. Gow, and C. T. Byrnes, Bayesian analysis of LIGO-Virgo mergers: Primordial vs astrophysical black hole populations, Phys. Rev. D **102**, 123524 (2020).

[36] G. Franciolini, I. Musco, P. Pani, and A. Urbano, From inflation to black hole mergers and back again: Gravitational-wave data-driven constraints on inflationary scenarios with a first-principle model of primordial black holes across the QCD epoch, Phys. Rev. D **106**, 123526 (2022).

[37] L. Liu, Z.-K. Guo, and R.-G. Cai, Effects of the merger history on the merger rate density of primordial black hole binaries, Eur. Phys. J. C **79**, 717 (2019).

[38] T. Nakamura, M. Sasaki, T. Tanaka, and K. S. Thorne, Gravitational waves from coalescing black hole MACHO binaries, Astrophys. J. Lett. **487**, L139 (1997).
[39] K. Ioka, T. Chiba, T. Tanaka, and T. Nakamura, Black hole binary formation in the expanding universe: Three body problem approximation, Phys. Rev. D **58**, 063003 (1998).
[40] P. C. Peters, Gravitational radiation and the motion of two point masses, Phys. Rev. **136**, B1224 (1964).
[41] B. Carr, S. Clesse, J. Garcia-Bellido, M. Hawkins, and F. Kuhnel, Observational evidence for primordial black holes: A positivist perspective, Phys. Rep. **1054**, 1 (2024).
[42] B. Carr, K. Kohri, Y. Sendouda, and J. Yokoyama, Constraints on primordial black holes, Rep. Prog. Phys. **84**, 116902 (2021).
[43] B. Carr and J. Silk, Primordial black holes as generators of cosmic structures, Mon. Not. R. Astron. Soc. **478**, 3756 (2018).
[44] J. Garriga, A. Vilenkin, and J. Zhang, Black holes and the multiverse, J. Cosmol. Astropart. Phys. 02 (2016) 064.
[45] H. Deng, J. Garriga, and A. Vilenkin, Primordial black hole and wormhole formation by domain walls, J. Cosmol. Astropart. Phys. 04 (2017) 050.
[46] Y.-T. Wang, Y. Cai, and Y.-S. Piao, Phase-transition sound of inflation at gravitational waves detectors, Phys. Lett. B **789**, 191 (2019).
[47] H.-H. Li, G. Ye, and Y.-S. Piao, Is the NANOGrav signal a hint of dS decay during inflation?, Phys. Lett. B **816**, 136211 (2021).
[48] M. Kleban and C. E. Norton, Monochromatic mass spectrum of primordial black holes, arXiv:2310.09898.
[49] R. Basu, A. H. Guth, and A. Vilenkin, Quantum creation of topological defects during inflation, Phys. Rev. D **44**, 340 (1991).
[50] S. R. Coleman and F. De Luccia, Gravitational effects on and of vacuum decay, Phys. Rev. D **21**, 3305 (1980).